FEBS Letters xxx (2007) xxx–xxx

Proton transfer in the photosynthetic reaction center of *Blastochloris viridis*

Maria A. Kozlova[a,b], Hanno D. Juhnke[c], Dmitry A. Cherepanov[d], C. Roy D. Lancaster[c], Armen Y. Mulkidjanian[a,b,*]

[a] *A.N. Belozersky Institute of Physico-Chemical Biology, Moscow State University, 119991 Moscow, Russia*
[b] *School of Physics, University of Osnabrück, 49069 Osnabrück, Germany*
[c] *Department of Molecular Membrane Biology, Max Planck Institute of Biophysics, 60438 Frankfurt am Main, Germany*
[d] *A.N. Frumkin Institute of Physical Chemistry and Electrochemistry, Russian Academy of Sciences, Moscow, Russia*

Received 30 October 2007; revised 27 November 2007; accepted 5 December 2007

Available online

Edited by Peter Brzezinski

Abstract Photosynthetic reaction centers of *Blastochloris viridis* require two quanta of light to catalyse a two-step reduction of their secondary ubiquinone Q_B to ubiquinol. We employed capacitive potentiometry to follow the voltage changes that were caused by the accompanying transmembrane proton displacements. At pH 7.5 and 20 °C, the Q_B-related voltage generation after the first flash was contributed by a fast, temperature-independent component with a time constant of ~30 μs and a slower component of ~200 μs with activation energy (E_a) of 50 kJ/mol. The kinetics after the second flash featured temperature-independent components of 5 μs and 200 μs followed by a component of 600 μs with $E_a \sim 60$ kJ/mol.

Keywords: Photosynthetic reaction center; Ubiquinone; Proton transfer; Capacitive potentiometry; *Blastochloris viridis*; *Rhodobacter sphaeroides*

1. Introduction

The photosynthetic reaction center (RC) is a pigment–protein complex that converts the energy of light into electrochemical energy (for reviews see [1–3]). As shown in Fig. 1A, the RC of the purple α-proteobacterium *Blastochloris viridis* (former *Rhodopseudomonas viridis*), the first membrane protein for which the X-ray structure has been obtained, is formed by two membrane subunits (L and M) being flanked by the H subunit from the cytoplasmic side of the membrane and by a tetraheme *c*-type cytochrome from the periplasmic side [4,5]. The excitation of the *Bl. viridis* RC by a flash of light triggers a charge separation followed by a picosecond electron transfer (ET) across the membrane, from the bacteriochlorophyll dimer *P* to a bound primary quinone Q_A (menaquinone-9). While the oxidized P is reduced by cytochrome *c*, the electron is transferred along the membrane plane to a loosely bound secondary quinone Q_B (ubiquinone-9, see Fig. 1B), and reduces it to a tightly bound semiquinone anion $Q_B^{\cdot-}$. The reduction of $Q_B^{\cdot-}$ by the next electron – e.g. after the second flash of light – yields a ubiquinol Q_BH_2 [6–8]. By using capacitive potentiometry, Dracheva and co-workers followed the electrogenic proton transfer (PT) that accompanied the reduction of Q_B to Q_BH_2 in the RCs of *Bl. viridis* incorporated into proteoliposmes [9]. They have reported a Q_B-related voltage generation with an apparent time constant (τ) of ~400 μs only in response to the second flash. Further detailed studies of the same reactions in *Rhodobacter sphaeroides* have shown, however, that already the $Q_B^{\cdot-}$ formation after the first flash is coupled with electrogenic proton transfer from the surface [10]. As well, the transfers of the second electron and the first proton to $Q_B^{\cdot-}$ after the second flash were found to be kinetically coupled in *Rb. sphaeroides* [11]. In *Bl. viridis,* however, the voltage generation with τ of 400 μs [9] has seemed to be slower than the corresponding ET with τ of 50 μs [7,8]. Here we revisited the problem of voltage generation in *Bl. viridis* by employing a specific inhibitor terbutryn to discriminate the reactions at the Q_B site.

2. Materials and methods

The *Bl. viridis* cells were grown and their RCs were purified as described elsewhere [12]. Proteoliposomes were prepared according to Ref. [13]. The flash-induced voltage generation was traced by capacitive potentiometry, as described in detail elsewhere [10,14]. Proteoliposomes were fused to a nitrocellulose film impregnated with the solution of 150 mg/ml soybean phosphatidylcholine (type II, Sigma) and 20 mg/ml ubiquinone-10 in *n*-decane. The voltage changes were monitored by a home-made electrometer-amplifier (constructed by N. Spreckelmeier) and digitalised on a Nicolet Pro-90 oscilloscope (point resolution 1 μs). The samples were equilibrated in the dark for 20 min before being illuminated by series of two consecutive saturating flashes of light with 1 s interval. A Surelite Nd:Yag laser (532 nm, FWHM 6 ns, Continuum, USA) was used as an excitation source. The dark adaptation time between the series was 5–10 min. The sign of the flash-induced voltage changes indicated that RCs incorporated into liposomes with their cytochromes pointing outside. In order to separate the Q_B related voltage signal from the total response, the traces obtained in presence of the Q_B site inhibitor terbutryn (10 μM) were point-by-point subtracted from those measured after the first and the second flash, respectively, without the inhibitor. All traces were normalized to the amplitude of the terbutryn trace at 2 μs after the flash, and this amplitude, *A*, was taken as 100% on estimating the relative amplitudes of difference traces. The kinetic traces were fitted with exponentials; all points were considered with equal weight. The Pluk software (kindly provided by Dr. Y. Kalaidzidis) and Microcal Origin 6.0 package (OriginLab, USA) were used. The incubation medium contained routinely

*Corresponding author. Address: School of Physics, University of Osnabrück, 49069 Osnabrück, Germany. Fax: +49 541 9692656.
E-mail address: amulkid@uos.de (A.Y. Mulkidjanian).

0014-5793/$32.00
doi:10.1016/j.febslet.2007.12.010

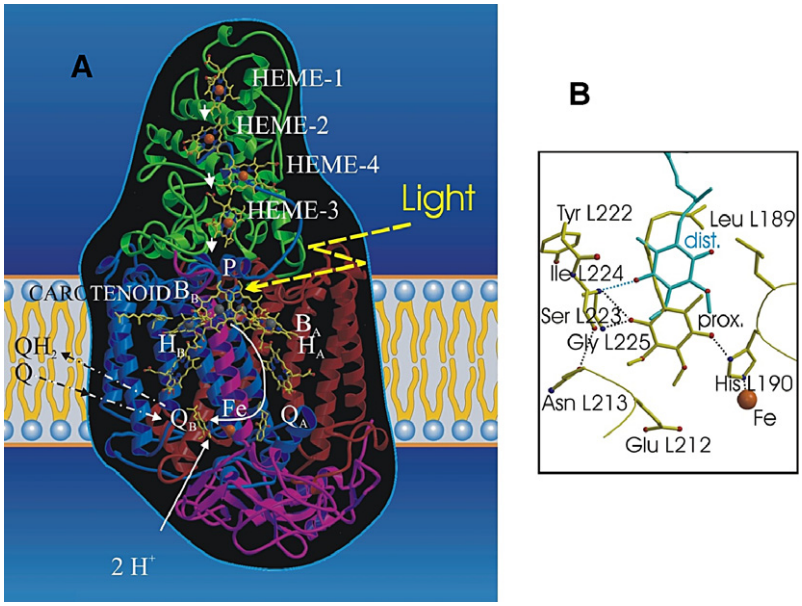

Fig. 1. Structure of the photosynthetic RC from *Blastochloris viridis*. (A) the structure of the *Bl. viridis* RC is represented schematically showing the heterotetramer of C, L, M, and H subunits as Cα traces in green, brown, blue, and purple, respectively, plus the 14 cofactors, which have been projected on to the molecule for better visibility. Also for the sake of clarity, the quinone tails are truncated after the first isoprenoid unit and the phytyl side chains of the bacteriochlorophyll and bacteriopheophytin molecules have been omitted, as have those atoms of the carotenoid molecule which were not observed in the electron density and assigned zero occupancy in the PDB entry 2PRC [20]. (B) Comparison of distal ($1PRC_{new}$, cyan) and proximal (2PRC, yellow) ubiquinone-binding sites [20].

20 mM HEPES, 100 mM KCl, 2 mM potassium ascorbate, 25 μM *N*,*N*,*N*′,*N*′-tetramethyl-*p*-phenylendiamine, and methylene blue, the concentration of which was optimized at each temperature and pH value to have O_B fully oxidized in 30 s [15]. To measure the pH-dependence, we used a pH–buffer mixture of Gly/GlyGly/potassium phosphate/potassium acetate (20 mM each).

3. Results and discussion

As shown in Fig. 2A, the flash-induced charge separation between P^+ and Q_A^- led to a kinetically unresolved voltage jump at <10 ns (see component A in Fig. 2A) followed by a slower rise. The rise could be due to electrogenic charge displacements both in the donor and in the acceptor parts of the RC [9]. However, only the voltage generation at the O_B site was expected to be sensitive to the Q_B antagonist terbutryn [16]. As shown in Fig. 2A, terbutryn partially suppressed the voltage rise both after the first and second flash. When the residual voltage rise in the presence of terbutryn (Fig. 2A) was resolved on a faster time scale (not documented), it was contributed by a component of <10 ns of the primary charge separation between P and Q_A, a component of ~200 ns making ~25% of

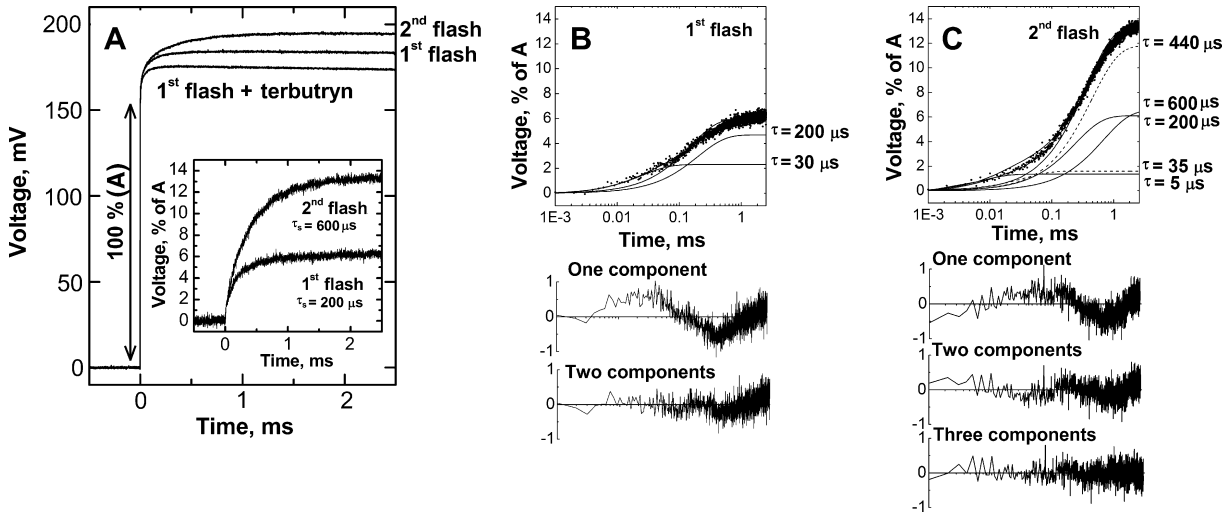

Fig. 2. Light-induced voltage generation in the RCs of *Blastochloris viridis* (pH 7.5, $T = 20$ °C). (A) Voltage traces as measured after the first and second flash, and after the first flash in the presence of Q_B-antagonist terbutryn. *Inset*: difference traces ±terbutryn reflecting the voltage changes at the Q_B site, as normalized to the charge separation component A. (B) Voltage generation after the first flash as approximated by one or two exponentials. The residuals of the fits are shown at the bottom of the plot. (C) voltage generation after the second flash as approximated by one, two or three exponentials. The components of the three exponential fit (5, 200 and 600 μs) are shown as solid lines. The components of the two exponential fit (440 and 35 μs) are shown as dashed lines.

the primary charge separation and attributable to ET from heme-3 of cytochrome *c* to P^+ (see Fig. 1), as well as a component of ~2 μs making 10% of the primary charge separation and owing to ET from heme-4 to heme-3, in good correspondence with data of Dracheva and co-workers who had studied these kinetic components in more detail [9]. These three steps of voltage generation are the same after each flash, so that they are nullified upon the calculation of the ±terbutryn difference traces (see Section 2 for the procedure). The difference traces, as obtained for the first and second flash, respectively, are shown in the inset to Fig. 2A; they reflect the voltage generation at the Q_B site upon $Q_B^{\cdot-}$ and Q_BH_2 formation [10,14]. In this work we focused on the kinetic analysis of these difference traces with the aim of understanding the proton transfer at the Q_B site of *Bl. viridis*.

As shown in Fig. 3A, the relative amplitude of the terbutryn-sensitive voltage generation after the first flash, in response to the semiquinone Q_B^- formation, depending on pH, made 2–8% of the charge separation A (see Section 2). Its kinetics could be approximated by two components that were well discernible at $t < 20$ °C (Figs. 2B and 3B). The faster component (~30 μs at 20 °C, pH 7.5) was virtually temperature-independent (see Table 1). The slower component (~200 μs at 25 °C) showed temperature dependence with apparent activation energy (E_a) of 50 ± 2 kJ/mol.

The relative amplitude of voltage generation after the second flash, in response to the Q_BH_2 formation, made 12–18% of charge separation A (see Fig. 3C). The kinetics featured a very fast component with an apparent τ of ~5 μs (20 °C, pH 7.5) and slower component(s) with τ of ~440 μs if fitted by a single exponential function. The double exponential fit of the slower component allowed better approximation with τ values of 200 and 600 μs at neutral pH and 25 °C (Figs. 2C and 3D). The 5 and 200 μs components were virtually temperature-independent (see Table 1). The slowest 600 μs component showed temperature dependence with E_a of 63 ± 5 kJ/mol.

Table 1
The activation energy (E_a) values calculated for the kinetics components of the voltage generation at the Q_B site after the first flash (ubisemiquinone formation) and second flash (ubiquinol formation), respectively, as measured in the range from 7 °C to 28 °C

Kinetics component	Very fast	Fast	Slow
E_a (*kJ/mol*)			
$Q_B \rightarrow Q_B^-$	–	<20 kJ/mol	50 ± 2 kJ/mol
$Q_B^- \rightarrow Q_BH_2$	<20 kJ/mol	<10 kJ/mol	63 ± 5 kJ/mol

Here we describe several new kinetic components of flash-induced voltage generation at the Q_B site of the *Bl. viridis* RCs. These novel components were apparently overlooked in the earlier pioneering study [9] because the difference between the voltage traces in response to the second and first flash was taken as a measure of Q_B-related voltage generation – under the apparently incorrect assumption of its absence after the first flash (cf. with Figs. 2A,B, and 3A,B).

The rates, relative amplitudes, as well as the pH- and temperature dependence of the voltage generation after the first flash (see Figs. 2B and 3A,C) resemble those reported for *Rb. sphaeroides* [10,14,17]. In *Rb. sphaeroides*, two kinetic

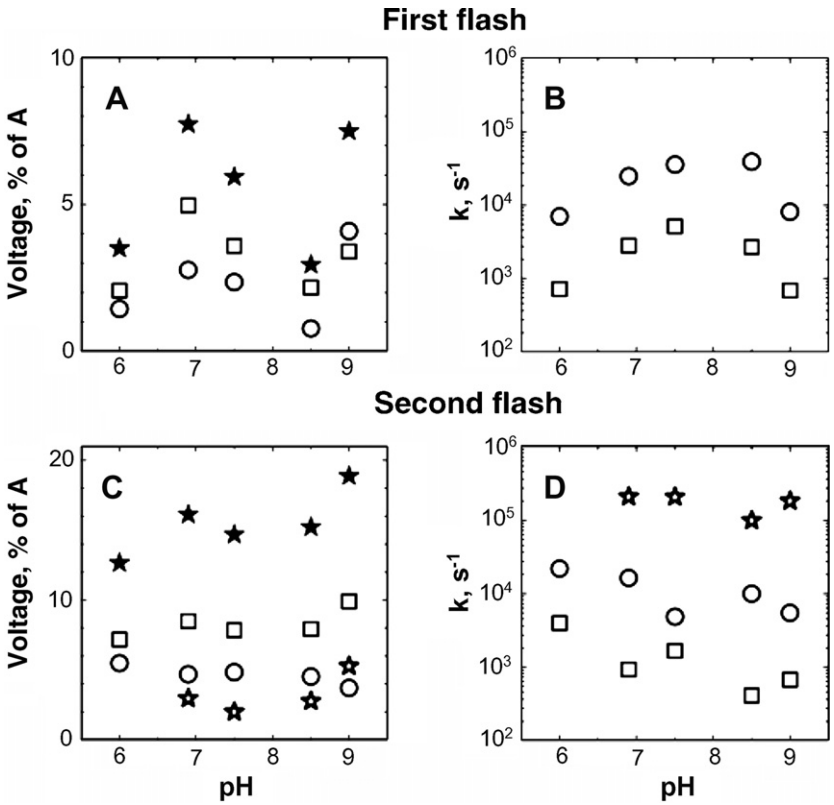

Fig. 3. Voltage generation at the Q_B site as function of pH. First flash: relative amplitudes (A) and time constants (B). Open circles: the 30 μs component, open squares: 200 μs component. Second flash: relative amplitudes (C) and time constants (D). Open stars: 5 μs component, open circles: 200 μs component, open squares: 600 μs component. The total amplitudes of the respective voltage changes are shown as filled stars.

components were discernable, namely a fast component with τ of ~80 μs and E_a of ⩽10 kJ/mol and a slow component with τ of ~500 μs at 10 °C and E_a of ~60–70 kJ/mol [14]. The E_a of the slow component was too large for PT proper and indicated a kinetic limitation by conformational change in a fraction of RCs. It was hypothesized that in some RCs Q_B may dwell in a remote non-functional site that is separated by a high activation barrier from the closer, catalytic position [14]. The low-temperature X-ray structures of the *Rb. sphaeroides* RC have indeed revealed two Q_B states, namely a remote "distal" position and a "proximal" one with Q_B being 5 Å closer to Q_A [18]. It has been argued that in the RCs with Q_B in a catalytic proximal position the proton redistribution towards Q_B^- proceeds with τ of ~100 μs and E_a < 10 kJ/mol whereas in the RCs with Q_B in a distal "stand-by" site, the formation of Q_B^- and the coupled proton displacements are limited by slow relocation of Q_B into the catalytic position [3,14,19]. Concurrently with the work on the *Rb. sphaeroides* RC, but using a different experimental strategy, distal and proximal positions (Fig. 1B) for the native Q_B species were found in the *Bl. viridis* RC [20]. Taking into account that the transfer of the first electron to Q_B takes ~20 μs in *Bl. viridis* [7], i.e. is somewhat faster than the components of voltage generation revealed here (cf. with Figs. 2B and 3B), the latter can be attributed, by analogy with *Rb. sphaeroides,* to the unimpeded and conformationally constrained proton redistribution upon the Q_B^- stabilization in *Bl. viridis*, respectively.

In *Bl. viridis*, the voltage generation in response to the second flash could be described by three kinetic components (see Figs. 2C and 3C, D). In the case of *Rb. sphaeroides*, the respective kinetics could be fitted by two kinetic components, namely a faster, almost temperature-independent one with τ of ~100 μs and a slower component with τ of ~500 μs at 20 °C and E_a of about 60 kJ/mol; these components were attributed to the first and second protonation of Q_B, upon the $Q_A^-Q_B^- \rightarrow Q_AQ_BH^-$ and $Q_AQ_BH^- \rightarrow Q_AQ_BH_2$ transitions, respectively [19,21,22]. The two faster components that were observed in *Bl. viridis* (with τ values of 5 and 200 μs) were weakly temperature dependent, whereas the slowest one displayed an E_a of about 50 kJ/mol (see Table 1). From the relative amplitudes of the components (see Fig. 3C) and by analogy with *Rb. sphaeroides*, the two faster components could be attributed to the first protonation of Q_B^-, while the slower one apparently reflects the second protonation.

Unlike the neutral Q_B, which can attain several positions in the Q_B site [20], the Q_B^- anion radical is attracted by the positively charged non-heme iron [23] and is expected, by analogy with the binding of a semiquinone-mimetic stigmatellin [20,24] and also by analogy with *Rb. sphaeroides* [14,18], to occupy a defined position in the pocket [20]. Therefore the heterogeneity of the voltage generation found upon the $Q_A^-Q_B^- \rightarrow Q_AQ_BH^-$ transition in *Bl. viridis* RCs is rather unexpected. It is noteworthy that the 5 μs component has never been observed with *Rb. sphaeroides* chromatophores either in the earlier works [10,21,22] or in the same high-resolution set-up [3] that was here used to investigate the RC of *Bl. viridis*. Another striking finding is that the 5 μs component of voltage generation is apparently faster than the reported time constant of ET from Q_A^- to Q_B^- after the second flash (~50 μs [7,8]). One possibility is that the 5 μs component reflects a terbutryn-sensitive charge displacement at the Q_B-site in response to Q_A^- formation. It has been shown that the formation of Q_A^- after the first flash triggers proton binding [25] and conformational changes [26] at the Q_B site of *Rb. sphaeroides*. Electrostatic calculations do not rule out that in *Bl. viridis* already the formation of Q_A^- can cause a prompt, electrogenic proton redistribution at the Q_B site [27]. Alternatively, the 5 μs component might reflect the heterogeneity in the kinetics of the second electron transfer in *Bl. viridis*. Unlike *Rb. sphaeroides*, the RCs of *Bl. viridis* have shown heterogeneity of their Q_A^- states, as inferred from the $Q_A^-P^+ \rightarrow Q_AP$ backreaction kinetics [28,29]. The heterogeneity was explained by the existence of two fractions of RCs becoming differently protonated in response to Q_A^- formation, and, accordingly, having different redox potentials of their Q_A/Q_A^- redox pairs [29]. According to Marcus theory [30], the ET from Q_A^- to Q_B has to be faster in the RCs with lower redox potential of the Q_A/Q_A^- pair. This low-potential fraction made about 20% in *Bl. viridis* RC preparation at neutral pH and increased upon alkalisation [28,29]. Hence, one can expect two kinetic components for the $Q_A^-Q_B^- \rightarrow Q_AQ_BH^-$ transition, with a faster component contributing 20% at neutral pH and increasing at higher pH values. These expectations, in principle, corroborate the pH-dependence of the relative amplitudes of the 5 μs and 200 μs components (see Fig. 3C).

In conclusion, the voltage generation at the Q_B site shows fundamental similarity in *Bl. viridis* and *Rb. sphaeroides*. At the same time, the kinetics of the first Q_B^- protonation after the second flash contain a novel minor 5 μs component that has no counterpart in *Rb. sphaeroides*. Further studies of site-specific mutants are needed to clarify the nature of this fast component.

Acknowledgements: Very useful discussions with Dr. W. Leibl are greatly appreciated. The research was funded by the Volkswagen Foundation, Max Planck Society, and by Grants from the Deutsche Forschungsgemeinschaft (Mu-1285/1, SFB 431-P15, SFB 472-P19, 436-RUS-113/210).

References

[1] Paddock, M.L., Feher, G. and Okamura, M.Y. (2003) Proton transfer pathways and mechanism in bacterial reaction centers. FEBS Lett. 555, 45–50.
[2] Cogdell, R.J., Gall, A. and Köhler, J. (2006) The architecture and function of the light-harvesting apparatus of purple bacteria: from single molecules to in vivo membranes. Quart. Rev. Biophys. 39, 227–324.
[3] Mulkidjanian, A.Y., Kozlova, M.A. and Cherepanov, D.A. (2005) Ubiquinone reduction in the photosynthetic reaction centre of *Rhodobacter sphaeroides*: interplay between electron transfer, proton binding and flips of the quinone ring. Biochem. Soc. Trans. 33, 845–850.
[4] Deisenhofer, J., Epp, O., Miki, K., Huber, R. and Michel, H. (1984) X-ray structure analysis of a membrane protein complex. Electron density map at 3 Å resolution and a model of the chromophores of the photosynthetic reaction center from *Rhodopseudomonas viridis*. J. Mol. Biol. 180, 385–398.
[5] Lancaster, C.R.D. (2007) Structures of Reaction Centers in Anoxygenic Bacteria in: Primary Processes of Photosynthesis. Principles and Apparatus. Part 2: Reaction Centers/Photosystems, Electron Transport Chains, Photophosphorylation and Evolution (Renger, G., Ed.), pp. 5–56, Royal Society of Chemistry, Cambridge.
[6] Shopes, R.J. and Wraight, C.A. (1985) The acceptor quinone complex of *Rhodopseudomonas viridis* reaction centers. Biochim. Biophys. Acta 806, 348–356.
[7] Leibl, W. and Breton, J. (1991) Kinetic properties of the acceptor quinone complex in *Rhodopseudomonas viridis*. Biochemistry 30, 9634–9642.

[8] Leibl, W., Sinning, I., Ewald, G., Michel, H. and Breton, J. (1993) Evidence that serine L223 is involved in the proton transfer pathway to Q_B in the photosynthetic reaction center of *Rhodopseudomonas viridis*. Biochemistry 32, 1958–1964.
[9] Dracheva, S.M., Drachev, L.A., Konstantinov, A.A., Semenov, A.Y., Skulachev, V.P., Arutjunjan, A.M., Shuvalov, V.A. and Zaberezhnaya, S.M. (1988) Electrogenic steps in the redox reactions catalyzed by photosynthetic reaction-center complex from *Rhodopseudomonas viridis*. Eur. J. Biochem. 171, 253–264.
[10] Drachev, L.A., Mamedov, M.D., Mulkidjanian, A.Y., Semenov, A.Y., Shinkarev, V.P. and Verkhovsky, M.I. (1990) Electrogenesis associated with proton-transfer in the reaction center protein of the purple bacterium *Rhodobacter sphaeroides*. FEBS Lett. 259, 324–326.
[11] Graige, M.S., Paddock, M.L., Bruce, J.M., Feher, G. and Okamura, M.Y. (1996) Mechanism of proton-coupled electron transfer for quinone (Q_B) reduction in reaction centers of *Rb. sphaeroides*. J. Am. Chem. Soc. 118, 9005–9016.
[12] Lancaster, C.R.D. and Michel, H. (1999) Refined crystal structures of reaction centres from *Rhodopseudomonas viridis* in complexes with the herbicide atrazine and two chiral atrazine derivatives also lead to a new model of the bound carotenoid. J. Mol. Biol. 286, 883–898.
[13] Kutuzov, M.A., Mamedov, M.D., Semenov, A.Y., Shinkarev, V.P., Verkhovsky, M.I., Abdulaev, N.G. and Drachev, L.A. (1991) Functioning of quinone acceptors in the reaction center of the green photosynthetic bacterium *Chloroflexus aurantiacus*. FEBS Lett. 289, 179–182.
[14] Gopta, O.A., Bloch, D.A., Cherepanov, D.A. and Mulkidjanian, A.Y. (1997) Temperature dependence of the electrogenic reaction in the Q_B site of the *Rhodobacter sphaeroides* photosynthetic reaction center: The $Q_A^- Q_B \rightarrow Q_A Q_B^-$ transition. FEBS Lett. 412, 490–494.
[15] Mulkidjanian, A.Y., Shinkarev, V.P., Verkhovsky, M.I. and Kaurov, B.S. (1986) A study of kinetic properties of the stable semiquinone of the reaction center secondary acceptor in chromatophores of nonsulfur purple bacteria. Biochim. Biophys. Acta 849, 150–161.
[16] Lancaster, C.R.D., Bibikova, M.V., Sabatino, P., Oesterhelt, D. and Michel, H. (2000) Structural basis of the drastically increased initial electron transfer rate in the reaction center from a *Rhodopseudomonas viridis* mutant described at 2.00-angstrom resolution. J. Biol. Chem. 275, 39364–39368.
[17] Brzezinski, P., Paddock, M.L., Okamura, M.Y. and Feher, G. (1997) Light-induced electrogenic events associated with proton uptake upon forming Q_B^- in bacterial wild-type and mutant reaction centers. Biochim. Biophys. Acta 1321, 149–156.
[18] Stowell, M.H.B., McPhillips, T.M., Rees, D.C., Soltis, S.M., Abresch, E. and Feher, G. (1997) Light-induced structural changes in photosynthetic reaction center: implications for mechanism of electron–proton transfer. Science 276, 812–816.
[19] Cherepanov, D.A., Krishtalik, L.I. and Mulkidjanian, A.Y. (2001) Photosynthetic electron transfer controlled by protein relaxation: analysis by Langevin stochastic approach. Biophys. J. 80, 1033–1049.
[20] Lancaster, C.R.D. and Michel, H. (1997) The coupling of light-induced electron transfer and proton uptake as derived from crystal structures of reaction centres from *Rhodopseudomonas viridis* modified at the binding site of the secondary quinone, Q_B. Structure 5, 1339–1359.
[21] Gopta, O.A., Cherepanov, D.A., Mulkidjanian, A.Y., Semenov, A.Y. and Bloch, D.A. (1998) Effect of temperature and surface potential on the electrogenic proton uptake in the Q_B site of the *Rhodobacter sphaeroides* photosynthetic reaction center: $Q_A^- Q_B^- \rightarrow Q_A Q_B H_2$ transition. Photosynth. Res. 55, 309–316.
[22] Cherepanov, D.A. et al. (2000) Reduction and protonation of the secondary quinone acceptor of *Rhodobacter sphaeroides* photosynthetic reaction center: kinetic model based on a comparison of wild-type chromatophores with mutants carrying Arg → Ile substitution at sites 207 and 217 in the L-subunit. Biochim. Biophys. Acta 1459, 10–34.
[23] Nonella, M. and Schulten, K. (1991) Molecular dynamics simulation of electron-transfer in proteins – theory and application to $Q_A \rightarrow Q_B$ transfer in the photosynthetic reaction center. J. Phys. Chem. 95, 2059–2067.
[24] Lancaster, C.R., Hunte, C., Kelley 3rd, J., Trumpower, B.L. and Ditchfield, R. (2007) A comparison of stigmatellin conformations, free and bound to the photosynthetic reaction center and the cytochrome bc_1 complex. J. Mol. Biol. 368, 197–208.
[25] Maroti, P., Hanson, D.K., Schiffer, M. and Sebban, P. (1995) Long-range electrostatic interaction in the bacterial photosynthetic reaction centre. Nat. Struct. Biol. 2, 1057–1059.
[26] Ginet, N. and Lavergne, J. (2001) Equilibrium and kinetic parameters for the binding of inhibitors to the Q_B pocket in bacterial chromatophores: dependence on the state of Q_A. Biochemistry 40, 1812–1823.
[27] Lancaster, C.R.D., Michel, H., Honig, B. and Gunner, M.R. (1996) Calculated coupling of electron and proton transfer in the photosynthetic reaction center of *Rhodopseudomonas viridis*. Biophys. J. 70, 2469–2492.
[28] Shopes, R.J. and Wraight, C.A. (1987) Charge recombination from the $P^+Q_A^-$ state in reaction centers from *Rhodopseudomonas viridis*. Biochim. Biophys. Acta 893, 409–425.
[29] Sebban, P. and Wraight, C.A. (1989) Heterogeneity of the $P^+Q_A^-$ recombination kinetics in reaction centers from *Rhodopseudomonas viridis* – the effects of pH and temperature. Biochim. Biophys. Acta 974, 54–65.
[30] Marcus, R.A. and Sutin, N. (1985) Electron transfers in chemistry and biology. Biochim. Biophys. Acta 811, 265–322.

Please cite this article in press as: Kozlova, M.A. et al., Proton transfer in the photosynthetic reaction center ..., FEBS Lett. (2007), doi:10.1016/j.febslet.2007.12.010